Quaternary Science Reviews 117 (2015) 113–123

Contents lists available at ScienceDirect

Quaternary Science Reviews

journal homepage: www.elsevier.com/locate/quascirev

Tree-ring footprints of drought variability in last ~300 years over Kumaun Himalaya, India and its relationship with crop productivity

Ram R. Yadav [a,*], Krishna G. Misra [a], Akhilesh K. Yadava [a], Bahadur S. Kotlia [b], Sandhya Misra [a,c]

[a] Birbal Sahni Institute of Palaeobotany, 53 University Road, Lucknow, 226007, India
[b] Centre of Advanced Study in Geology, Kumaun University, Nainital, 263002, India
[c] Indian Institute of Technology Gandhinagar, Ahmedabad, 382424, India

ARTICLE INFO

Article history:
Received 10 September 2014
Received in revised form
25 March 2015
Accepted 2 April 2015
Available online

Keywords:
Himalayan cedar
Tree-ring
Standardized Precipitation Index
Drought
Rabi crop
Agriculture
Kumaun Himalaya
India

ABSTRACT

We reconstructed Standardized Precipitation Index (SPI), a metric of drought, using tree-ring width chronologies of Himalayan cedar (*Cedrus deodara* (Roxb.) G. Don) prepared from two ecologically homogeneous settings in the Kumaun Himalaya, India. The reconstruction employing first principal component of the two site chronologies in linear regression model helped in extending 7-month SPI of May (SPI7-May) back to 1720 CE. The calibration model capturing 60% of variance in the observed SPI series (1902–1967) is the strongest so far from the Indian region. On achieving such a robust tree-ring calibration we are of the opinion that SPI should provide a better option to develop long-term drought records for the data scarce Himalayan region. The SPI reconstruction revealed high year-to-year variability with 1816 (SPI −1.92) and 1737 (SPI +2.33) the driest and the wettest years respectively. The five year mean of reconstructed SPI revealed multiyear droughts in 1920–1924, 1782–1786, 1812–1816, 1744–1748, 1964–1968 and pluvial phases in 1911–1915, 1723–1727, 1788–1792, 1758–1762 and 1733–1737.

The SPI7-May was found to be significantly correlated with wheat-barley productivity data of Almora in Kumaun, close to our tree ring sites ($r = 0.60$, two-tailed $p < 0.0001$). However, we observed that the wheat-barley productivity data, to some extent, were better correlated with 7-month SPI of April (SPI7-April) ($r = 0.69$, two-tailed $p < 0.0001$). The difference in relationship of wheat-barley productivity and SPI of above two periods is largely due to the prevailing crop phenology in the region. The wheat and barley crops sown in October–November are usually harvested in May when the Himalayan cedar trees are in active vegetation phase of seasonal growth in Almora region. We observed strong and significant correlation in SPI7-May and SPI7-April ($r = 0.75$, two-tailed $p = 0.0001$) underpinning that the tree-ring derived SPI7-May could also be taken as a proxy of wheat-barley production in Almora region. This observation also stands for the past as we noted that most of the droughts recorded in our reconstruction (SPI <1) were associated with rabi crop failures in the Kumaun Himalaya. The findings of this study establish that the SPI7-May developed from tree rings should serve as an important base line data to quantify the impact of droughts on forest as well as rabi crop productivity in hilly terrains of the Kumaun Himalaya in long-term perspective.

1. Introduction

Drought is a naturally occurring subtle climatic phenomenon that may persist for a season or multiple years and affects more population than any other natural hazard (Wilhite, 2000). In India, National Commission on Agriculture (GOI, 1976) classified droughts in three categories as meteorological, hydrological and agricultural droughts. The agricultural drought is a situation when rainfall and soil moisture are inadequate during the crop growing season to support healthy crop growth to maturity. Recurring droughts in one or the other region of India are known to critically affect the livelihood of the vast majority of low income people whose sustenance is dependent on agriculture (Mishra and Singh, 2010; Gupta et al., 2011). Nearly 79.44 million ha of agricultural land area constituting ~57% of the cultivated area is rainfed and contributes 44% of the total food grain production in India (Anonymous, 2009). Such

* Corresponding author.
E-mail address: rryadav2000@gmail.com (R.R. Yadav).

http://dx.doi.org/10.1016/j.quascirev.2015.04.003
0277-3791/

an extensive rainfed agriculture system practiced in India ranking first among the rainfed agricultural countries in the world, both in extent and value of produce (Aggarwal, 2013), makes economy of the country much dependent on seasonal distribution of rainfall. As nearly half of the total workforce in India (~52%) is still employed by the farm sector, severe droughts affecting agriculture productivity seriously hamper the developmental pathways of the country (Gadgil and Kumar, 2006). Such challenges are far bigger in the Himalayan region of India where drought impacts are high due to poor irrigation infrastructure facilities. The terrain constrains in the Himalaya hinder the development of sufficient crop irrigation facilities, making agriculture highly vulnerable to natural rainfall patterns. In view of this a better understanding of drought behaviour in long-term perspective is very important to develop appropriate climate adaptive measures.

The high-resolution proxy climate records used to extend the weather data back in the historical past provide valuable window to understand climate variability under the backdrop of anthropogenic changes (IPCC, 2013). The tree-ring records from moisture stressed sites in different parts of the world have been successfully used to understand temporal and spatial patterns of droughts (Woodhouse and Overpeck, 1998; Cook et al., 2004, 2007; Touchan et al., 2005, 2008, 2011; Esper et al., 2007; Stahle et al., 2007, 2013; Woodhouse et al., 2010; Burnette and Stahle, 2013; Griffin and Anchukaitis, 2014). Recently, a considerable progress has been also made towards this direction to develop annually resolved tree-ring-based drought/hydrological records for semi-arid to arid regions of Asia (Sheppard et al., 2004; Davi et al., 2006; Li et al., 2006, 2007; Liang et al., 2006; Treydte et al., 2006; Yin et al., 2008; Cook et al., 2010; Shao et al., 2010; Zhang et al., 2011; Ram, 2012; Sano et al., 2012; Yang et al., 2012, 2014a, b; Sun and Liu, 2013; Yadav, 2013). The age of many long living conifer species growing in semi-arid to arid regions of the western Himalaya are found to exceed over millennium (Esper, 2000; Cook et al., 2003; Singh et al., 2004; Yadav et al., 2006; Singh and Yadav, 2007; Yadav, 2012). Precisely dated annually resolved tree-ring chronologies of such old trees from semi-arid to arid regions of the western Himalaya should provide a valuable archive of drought variability in long-term perspective.

To understand the relative strength of droughts various types of indices have been devised over times (Keyantash and Dracup, 2002) and amongst these the Palmer Drought Severity Index (PDSI; Palmer, 1965) is widely used. However, realizing the fact that droughts vary over different timescales depending on the response times of different meteorological, hydrological, agricultural and socioeconomic systems, and PDSI having a fixed temporal scale, multi-scalar drought indices such as Standardized Precipitation Index (SPI; Mckee et al., 1993) and Standardized Precipitation Evapotranspiration Index (SPEI; Vicente-Serrano et al., 2010) have come in to use recently. The SPI is being widely used to monitor short-term water supplies such as soil moisture which is important for agriculture production, as well as long-term water resources such as groundwater supplies, stream flow and reservoir levels (Mishra and Singh, 2010). However, in assessment of agriculture droughts the SPI has its own limitation as the availability of soil moisture is directly controlled by evapotranspiration, which is not taken into account in derivation of SPI. In spite of the above limitation we used SPI data in present study, as it was calculated from precipitation records available from weather stations close to our tree-ring sites in the western Himalaya. The SPI was also preferred for reconstruction over the other drought indices, viz., PDSI and SPEI as it showed statistically much robust calibrations with the tree-ring width chronologies of Himalayan cedar. Recently, the World Meteorological Organization in 2009 (WMO, 2012) also recommended that SPI, in addition to other drought indices, should be used as a drought metric by all National Meteorological and Hydrological Services around the world to characterise the meteorological droughts. The SPI reconstruction presented here-in is the first attempt to develop drought records for the Kumaun (Kumaon) Himalaya, India using tree-ring data of Himalayan cedar. The SPI records were also used to understand relationship with crop productivity in the rainfed agricultural region of Almora, adjacent to tree-ring locations.

2. Data and methods

2.1. Tree-ring data

Himalayan cedar commonly grows in semi-arid to arid regions of the Indian Himalaya. Good amount of winter snowpack, not too heavy summer monsoon rainfall and well drained soils are its primary ecological requirement. Over humid sites, the tree age is usually limited to only a few hundred years due to frequent wood rot, but in drier locations the age of many conifer species have been found to extend over the last millennium and even more (Singh et al., 2004). Due to the ecological preferences of Himalayan cedar for semi-arid and arid conditions the dendrochronological series of this species are found to be very sensitive indicators of variations in drought (Yadav, 2013). In the present study increment core samples of Himalayan cedar growing in Jageshwar and Gangolihat in the Kumaun region collected in May 2013 were used (Fig. 1). The Himalayan cedar in the Kumaun Himalaya is not native and was introduced in temple complexes several centuries ago depending on the establishment of religious shrines. The age of introduced Himalayan cedar in the Kumaun Himalaya using dendrochronological methods has been estimated back to the early 16th century CE (Yadav et al., 2014a, b). Due to suitable environmental conditions the Himalayan cedar introduced in the Kumaun region has completely naturalized and is showing very good regeneration. The sampled trees, used in this study, were found growing on sites with thin soil cover and variable slopes on northwest aspect where the ground water balance does not seem to have much impact on tree growth. Thin soil conditions and slope gradients favour fast run-off of the meteoric water to down streams making trees susceptible to soil moisture deficit. The increment core samples of Himalayan cedar collected from Jageshwar and Gangolihat sites in the Kumaun Himalaya (Fig. 1) were processed following conventional dendrochronological methods and growth ring sequences precisely dated to calendar year of their formation (Fritts, 1976). The ring widths of crossdated samples were measured to 0.01 mm resolution using linear encoder (LINTAB) coupled with personal computer (Rinn, 1996). To understand temporal growth dynamics in tree-ring series ring-width measurement plots from both the sites were carefully studied. The ring-width plots of tree samples from two sites revealed that the Himalayan cedar growth was influenced by stand dynamic features such as changing competition due to gap formations created by falling of adjacent trees. Therefore, to maximize the common signal in tree-ring-width chronologies, we detrended the measurement series by using 50-year cubic spline with a 50% frequency response function cut off (Cook and Peters, 1981). The ring-width series of individual tree samples were power transformed prior to detrending to stabilize variance in the heteroscedastic tree-ring-width measurement series (Cook and Peters, 1997). The growth trends were removed from the power transformed individual measurement series by subtraction that minimizes the end fitting-type bias as compared to the ratios (Cook and Peters, 1997). In order to reduce the influence of outliers the detrended ring-width measurement series of respective trees were averaged to a mean chronology (standard) by computing the biweight robust mean

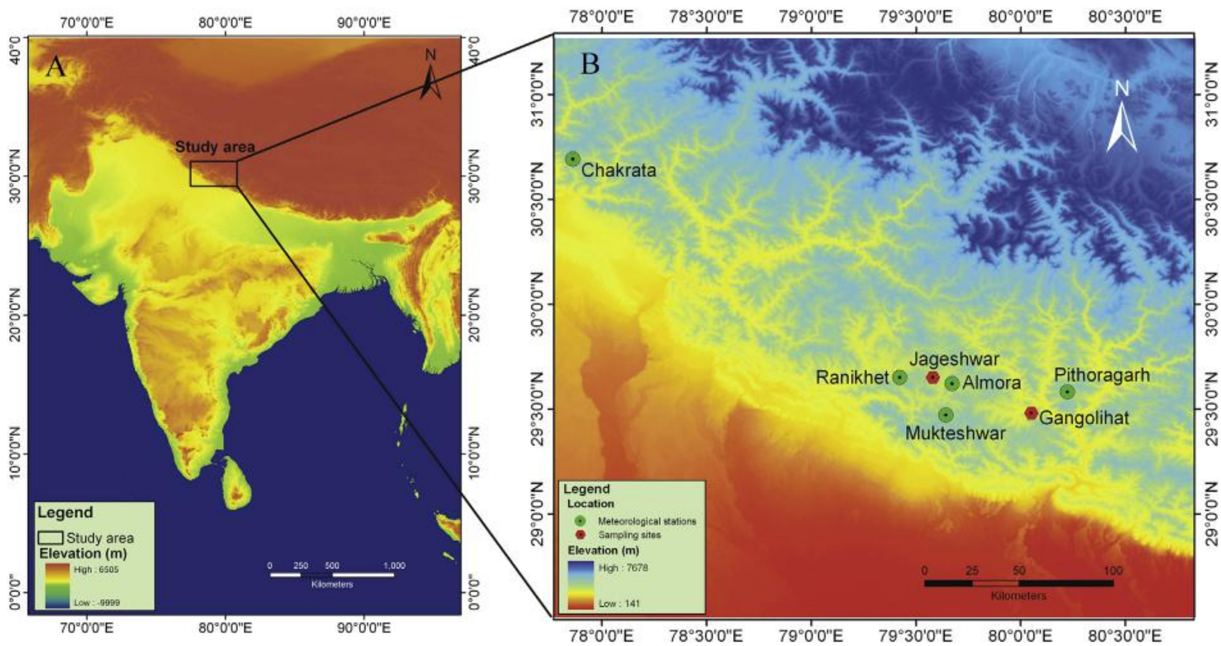

Fig. 1. Map showing the locations of the tree ring sampling sites of the Himalayan cedar and meteorological stations; A. General view of the study area, B. Location of tree-ring sites and weather stations used in the study.

(Cook, 1985). The other set of chronology (residual) was also prepared where low-order autocorrelation from detrended series was removed using autoregressive moving average (ARMA) modelling and the resulting residual series averaged to a mean site chronology by computing the biweight robust mean (Cook, 1985). The replication of 12 and 15 tree samples in Jageshwar and Gangolihat site chronologies respectively were found to be sufficient to achieve threshold expressed population signal (eps) level of 0.85 (Wigley et al., 1984). The residual chronology statistics of two sites are shown in Table 1. The two site residual chronologies with eps level >0.85 showed significant correlation for the common period 1720–2012 CE ($r = 0.75$, two-tailed $p < 0.0001$) underpinning common environmental forcing affecting growth dynamics of trees over the respective sites.

2.2. Climate data

Weather records from Kumaun, analogous to that in other regions of the western Himalaya, are spatially and temporally restricted. The longest weather record (temperature and precipitation) available for Mukteshwar (29° 28′ N–79° 38′ E, 2171 m asl) in Nainital, Uttarakhand, close to the tree-ring sampling sites extends back to 1897. The weather data of Mukteshwar show that the bulk of precipitation (~73% of 1270 mm annual) occurs in monsoon season spread over June–September (Fig. 2). The November–May precipitation occurring largely due to western disturbances is ~22% of the annual precipitation. In our previous studies (Yadav et al., 1999; Yadav and Singh, 2002; Yadav et al., 2004, 2011; Yadav, 2011a, b), we observed that due to high spatial variability in precipitation in the orography dominated western Himalayan region single station data, which do not represent the regional climate features, are not suitable for calibration of tree-ring chronologies. In view of this we prepared a regional mean precipitation series by merging homogeneous data sets of five weather stations (Table 2) available from locations close to the tree-ring sampling sites. Averaging of multiple station data series helps in minimizing the effect of site specific micro-climatic variations and maximization of regional and larger-scale climate features in the mean series. The merging of precipitation data of five stations as mentioned above was also guided by the existence of good year-to-year coherence in precipitation data and the existence of significant correlations. However, we observed relatively stronger year-to-year coherence and significant correlations in precipitation of different stations during the non-monsoon months as compared to summer monsoon season (June–September) (Table 3, Fig. 3). The monthly precipitation data of these five stations after normalization with reference to 1901–1967 common period were merged to prepare the regional mean monthly series, however, the precipitation series from 1968 to 2011 consisted single station data of only Mukteshwar. The regional mean monthly normalized precipitation series were then converted to actual precipitation with respect to the mean monthly precipitation and mean standard deviation of all five stations.

The temperature records from the Kumaun region available with us for present study were only of Mukteshwar station (1897–1991). The mean monthly temperature data show that June

Table 1
Chronology (residual) statistics of Himalayan cedar from two sites in Kumaun. SY- start year of the chronology, EPS-expressed population signal, MI-mean index, MS-mean sensitivity, SD–standard deviation, AR1-first order autocorrelation.

S. No.	Site	Location	Elevation (m)	Aspect	Cores/trees	SY	Chronology with EPS >0.85	MI	MS	SD	AR1
1	Gangolihat	29°39′N-80°01′E	1760	Northwest	38/27	1668	1720–2012	0.998	0.194	0.170	0.00
2	Jageshwar	29°38′N-79°51′E	1851	northwest	41/37	1536	1690–2012	0.992	0.248	0.213	0.00

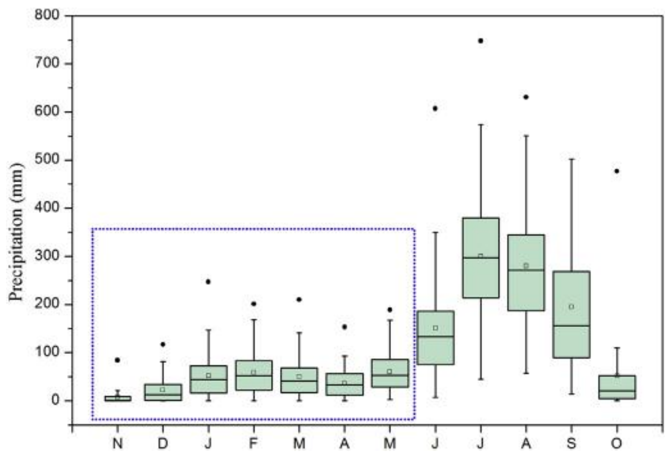

Fig. 2. Monthly precipitation variations over Kumaun, the western Himalaya. November–May are dry months with very low precipitation. The figure is based on Mukteshwar meteorological station mean precipitation data.

is the hottest month of the year with mean temperature ~18.4 °C and January the coldest with mean temperature ~5.4 °C at Mukteshwar.

2.3. Climate signal in tree-ring data

To understand climate signal present in tree-ring data the residual version of two site chronologies were used in Pearson correlation analyses with monthly climate variables (monthly total precipitation and mean monthly temperature) from October of the previous year to October of the current year. The October, being usually the end of growing season was also taken into analysis with the consideration that the radial growth of trees might continue if the climatic conditions are favourable enough for growth during this month. For correlation analyses temperature data of Mukteshwar (1897–1991) and regional mean precipitation data representing five station mean from 1901 to 1967 and only of Mukteshwar from 1968 to 1991 were used. We performed bootstrapped correlation analyses using software DENDROCLIM2002 (Biondi and Waikul, 2004) for 1901–1991 for which both precipitation and temperature data were available with us (figure not shown). In correlation analyses it was observed that the precipitation from previous year October to current year May showed direct relationship with the respective site chronologies, with consistently positive and significant correlations (two tailed $p < 0.05$) from February–May. The precipitation during summer monsoon months (June–September), when it is prevalent in the region due to active southwest summer monsoon, did not show significant correlation. However, in case of temperature the residual version of two site chronologies showed negative relationship with mean monthly temperature of Mukteshwar for most of the months except from July–October when it turned positive. The

Table 2
Meteorological stations used in preparing the mean regional precipitation series and SPI.

S. No.	Station	Latitude (N)	Longitude (E)	Altitude (m)	Length of record
1	Almora	29°37′	79°40′	1651	1901–1967
2	Chakrata	30°41′	77°52′	2118	1901–1967
3	Mukteshwar	29°28′	79°38′	2171	1897–2011
4	Pithoragarh	29°35′	80°13′	1514	1901–1967
5	Ranikhet	29°39′	79°25′	1869	1901–1968

Table 3
Pearson correlation in precipitation of non-monsoon (previous year October to current year May (OM)) in bold letters and monsoon (June–July–August–September (JJAS)) in italics of stations used in this study (1902–1967). Levels of significance are given in parentheses.

Station		Chakrata	Mukteshwar	Pithoragarh	Ranikhet
Almora	OM	**0.69 (0.0001)**	**0.90 (0.0001)**	**0.73 (0.0001)**	**0.91 (0.0001)**
	JJAS	*0.71 (0.0001)*	*0.45 (0.0001)*	*0.50 (0.0001)*	*0.80 (0.0001)*
Chakrata	OM		**0.63 (0.0001)**	**0.42 (0.0004)**	**0.70 (0.0001)**
	JJAS		*0.35 (0.004)*	*0.47 (0.0001)*	*0.77 (0.0001)*
Mukteshwar	OM			**0.75 (0.0001)**	**0.88 (0.0001)**
	JJAS			*0.41 (0.0006)*	*0.52 (0.0001)*
Pithoragarh	OM				**0.75 (0.0001)**
	JJAS				*0.58 (0.0001)*

correlation analyses revealed that cool-moist conditions over an extended period from previous year October to current May directly affects the radial growth of Himalayan cedar in the Kumaun Himalaya. Similar to our findings, precipitation accumulated during winter and spring seasons in arid zones in different geographic regions have also been found to be a dominant environmental variable controlling the inter-annual variability of tree growth (Meko et al., 2011; Stahle et al., 2013; Black et al., 2014). The first principal component (PC#1) of the two site residual chronologies with the Eigen value 1.752 explaining 87.6% of the variance in the common chronology period 1720–2012 CE also revealed relationship with monthly climate variables (Fig. 4) similar to that observed with independent chronologies.

The tree growth-climate relationship analyses presented here revealed that Himalayan cedar growth around the studied sites is governed by both precipitation and temperature. The correlation between tree-ring indices with precipitation and temperature nearly represent the mirror image of each other (Fig. 4) endorsing that soil moisture availability is very important in modulating the yearly growth of Himalayan cedar in Kumaun. Considering these findings we analysed relationship between tree-ring chronologies and drought indices, viz., Palmer Drought Severity Index (PDSI; Palmer, 1965) and Standardized Precipitation Evapotranspiration Index (SPEI; Vicente-Serrano et al., 2010). The monthly PDSI dataset developed by Dai et al. (2004) with a resolution of 2.5° × 2.5° grid point and available for the grid nearest to our sampling sites (27.5°–30°N and 77.5°–80°E) were used in correlation analyses with the residual version of tree-ring-chronologies. We observed that the correlation between tree-ring chronologies and monthly PDSI variables in most of the months was not statistically significant. The SPEI data of different temporal scales available via climate explorer (http://climexp.knmi.nl) on a 0.5° × 0.5° grid point were also used to study correlation with tree-ring chronologies. The SPEI data of 4–8 months time-scales for two grid points (29°–29.5°N and 79°–79.5°E; 30°–30.5°N and 79.5°–80°E) were used in correlation analyses with the tree-ring chronologies. We observed that 4-month SPEI of May showed statistically significant correlation with the tree-ring chronologies. However, the correlation between tree-ring chronologies and SPEI indices were observed to be much weaker than those observed with the regional monthly precipitation data alone. Considering this, we analysed relationship between tree-ring chronologies and Standardized Precipitation Index (McKee et al., 1993), a multi-scalar drought index developed using regional mean precipitation data series prepared for this study.

2.3.1. Precipitation data and SPI calculation

The computation of SPI for any location is based on the available long-term precipitation record. This long-term precipitation record is fitted to a gamma probability distribution function, which is then transformed into a normal distribution with mean of zero and

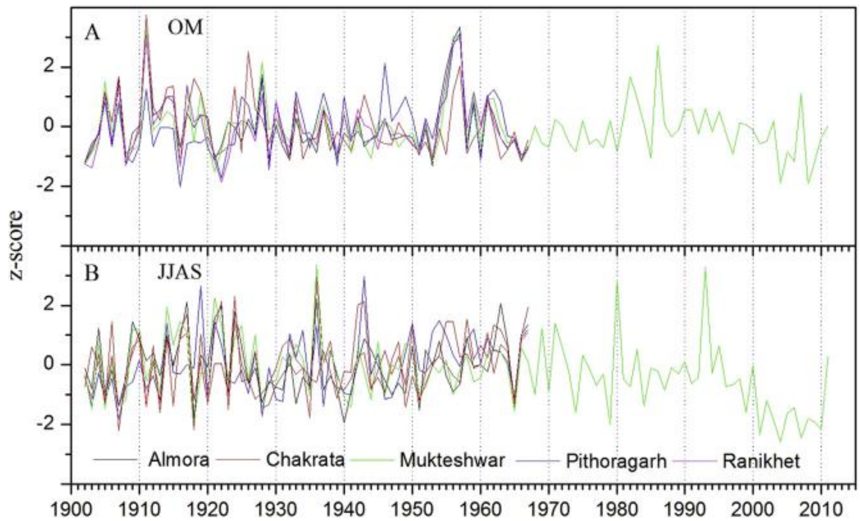

Fig. 3. Normalized seasonal precipitation over five weather stations used in this study. The data were normalized with respect to the 1902–1967 mean; A. October–May precipitation, B. June–September precipitation.

standard deviation unity (McKee et al., 1993; Edwards and Mckee, 1997). A full description on methods and equations for calculating the SPI are available in Lloyd-Hughes and Saunders (2002). In our present study we calculated SPI using regional precipitation series developed after merging five station precipitation data from the Kumaun Himalaya (Table 2). The regional precipitation series spanning over 1901–1967 was used to develop SPI of different temporal scales varying from one to nine months. The SPI of Mukteshwar data from 1968 to 2011 was also calculated for use in verification of the reconstruction. The SPI on such timescales is expected to reflect moisture availability affecting the growth of forest trees as well as agricultural crops. The positive SPI values indicate precipitation greater than the median value and negative values point to less than median precipitation. An event is treated as drought when SPI is continuously negative reaching intensity of −1.0 or less and opposite to this as wet.

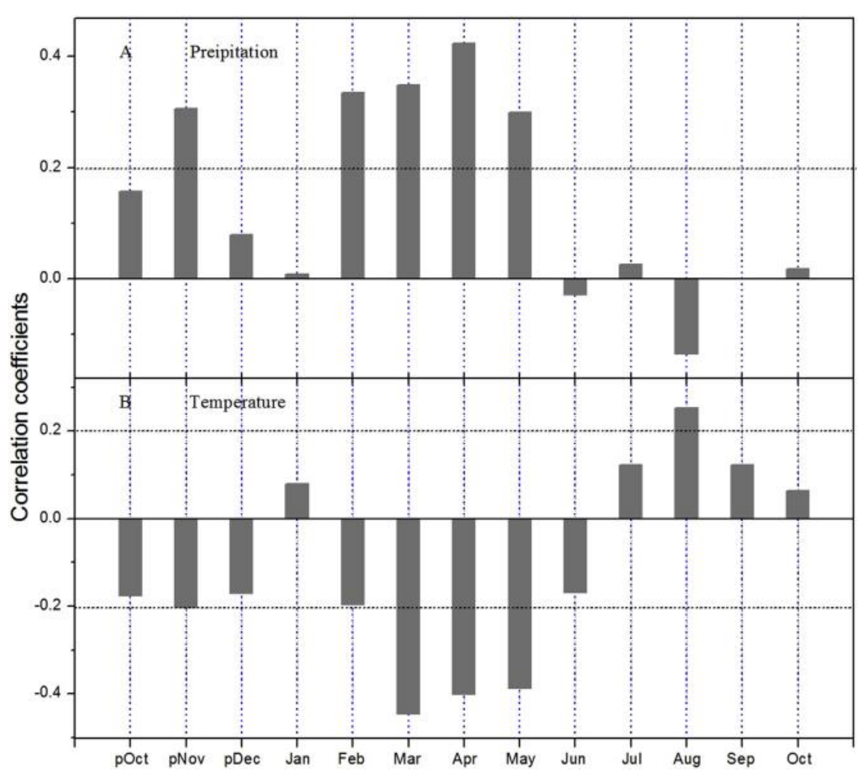

Fig. 4. Correlation functions of the first principal component (PC#1) of the residual chronologies of the Himalayan cedar from two sites with climate data; A. with monthly precipitation and B. with mean monthly temperature. The mean regional precipitation data prepared by merging five station data and mean monthly temperature of Mukteshwar were used in the analyses. (Dotted lines show 95% confidence level).

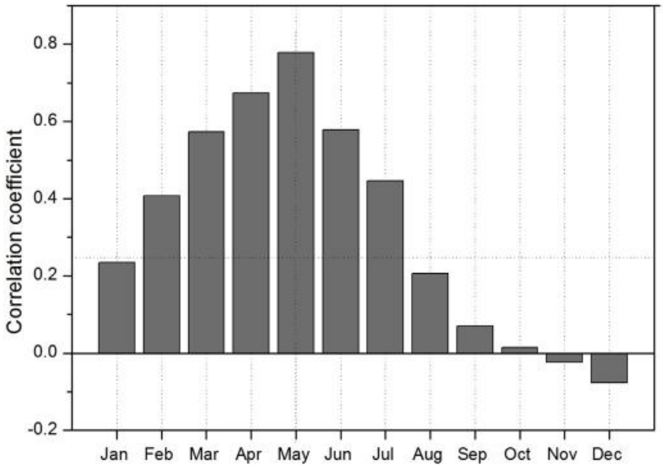

Fig. 5. Correlation functions of the PC#1 with 7-month SPI calculated for 1902–1967. The dotted line shows 95% confidence level.

2.4. Rabi crop productivity data

The wheat (*Triticum aestivum*) and barley (*Hordeum vulgare*) are the most important winter cereals of India. In hilly regions, these crops are normally sown in October/November and harvested in May/June and their success mainly depends on the distribution of rainfall during these months. Although in recent times, high yielding hybrid varieties of wheat have been developed for growing in the Indian plains, traditional varieties are still sown in the northern hill zones (Nagarajan, 2005). To understand recent trends in crop productivity we obtained wheat and barley production data of Almora in Kumaun with the courtesy of Agriculture Departments of Uttarakhand and Uttar Pradesh. The annual records of wheat and barley production procured by us from the respective government agriculture departments extended from 1974 to 2010. The production of wheat in Almora for 1974–2010 ranged from 520 to 1220 kg/ha (mean 961.8, standard deviation 175.2) and barley from 410 to 1260 kg/ha (mean 948.9, standard deviation 197.4). To understand the impact of droughts on crop productivity in log-term perspective we also used rabi crop failures recorded in archives for the rainfed agriculture regions of Almora. In our analyses of relationship between SPI and crop productivity the wheat and barley productivity data (1974–2010) were normalized relative to whole period mean and standard deviation.

2.5. Drought index (SPI) reconstruction

The analyses performed to understand relationship between tree-ring chronologies and climate variables in association with the similar studies performed earlier (Yadav et al., 2014a, b) suggest that the precipitation changes in premonsoon season are very important for the radial growth of Himalayan cedar trees over moisture stressed sites in the western Himalaya. In view of this we studied relationship between PC#1 of the residual chronologies of Himalayan cedar and SPI calculated for different timescales from one to nine months. The correlation study revealed strongest relationship between PC#1 and SPI7-May (Fig. 5). Due to the existence of such a high and significant correlation between SPI and PC#1 we performed calibration and reconstruction of SPI7-May using linear regression approach. For this, we first performed calibration/verification tests using SPI data prepared from regional mean precipitation data series (1902–1967). The split period calibration/verification tests were performed in two sub-periods, 1902–1932 and 1933–1967. The two sub-period (1902–1932, 1933–1967) calibration and verification statistics such as the reduction of error (RE), coefficient of efficiency (CE), Sign test, and Pearson correlation coefficient (Fritts, 1976; Cook and Kairiukstis, 1990) were used to test the fidelity of the reconstruction models (Table 4, Fig. 6). The robustness of the models underpinned by positive values of both the RE and the CE, which are the most rigorous test of model validation, denotes significant statistical skill in the reconstruction. On establishment of the veracity of calibration/verification statistics, we used 1902–1967 calibration for SPI reconstruction, which captured 60% of the variance in the instrumental SPI7-May data and the model, in terms of calibration statistics, is the strongest thus far reported from the Indian region. The reconstructed series revealed close year-to-year similarity and significant correlation with SPI7-May in different sub-periods ($r = 0.78$, 1902–1967, two-tailed $p < 0.0001$; $r = 0.70$, 1902–2011, two-tailed $p < 0.0001$). The correlations were also found statistically significant between reconstructed SPI and SPI data calculated using single station precipitation data of Mukteshwar ($r = 0.64$, 1968–2011, two-tailed $p = 0.0001$).

3. Results and discussion

3.1. Analyses of SPI reconstruction

The SPI7-May reconstruction spanning from 1720 to 2012 CE for the Kumaun Himalaya revealed high year-to-year variability (Fig. 7). The annual SPI7-May records (Table 5) show that 1816 was the driest year (SPI −1.92) and 1737 the wettest (SPI +2.33). The impact of such droughts on socioeconomic system can be devastating if drought similar to the magnitude of 1816 happens to recur in near future as resource demands have increased many folds now due to the burgeoning human population. The drought of 1816 coincides with the Tambora volcanic eruption, which is associated with the most destructive episode of abrupt climate change in modern historical record (Self et al., 2004). The unusual extreme weather in 1816 caused poor agricultural yields and outbreak of diseases like cholera and typhus in several mid-latitude south Asian countries and different parts of the world (Pisek and Brázdil, 2006). Large part of India also experienced unprecedented climate anomalies in 1816 with erratic summer monsoon and severe droughts (Jameson, 1820). Climate model studies have also revealed

Table 4
Calibration, verification statistics of SPI7-May reconstruction; ar^2-r^2 adjusted after degrees of freedom, R- Pearson correlation, Sign test, RE (reduction of error) and CE (coefficient of efficiency) (Fritts, 1976; Cook and Kairiukstis, 1990). Levels of significance are indicated in parentheses.

S. No.	Period	Number of series	Calibration		Verification				
			Period	ar^2 (%)	Period	R	Sign test	RE	CE
1	1730–2012	2	1902–1932	64	1933–1967	0.73 (0.0001)	$25^+/10^-$ (0.0167)	0.429	0.428
			1933–1967	52	1902–1932	0.81 (0.0001)	$28^+/3^-$ (0.0000465)	0.597	0.597
			1902–1967	60	1968–2011	0.64 (0.0001)	$32^+/12^-$ (0.00366)	0.360	0.357
			1968–2011	40	1902–1967	0.78 (0.0001)	$50^+/16^-$ (0.0000333)	0.416	0.413
			1902–2011	48					

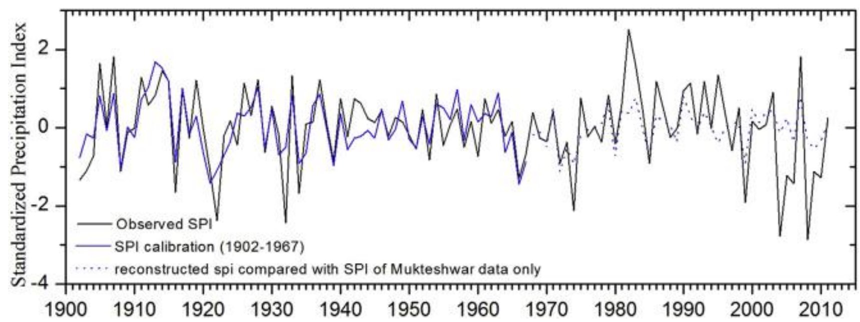

Fig. 6. Observational and reconstructed SPI7-May plotted together for comparison (1902–1967 calibration period was used in reconstruction).

decrease in summer monsoon rainfall over India in response to Mount Pinatubo eruption in 1991 (Joseph and Zeng, 2009), however, there are regional and seasonal differences in volcanic forcing on climate (Robock, 2000). The tree-ring data from semi-arid and arid regions of the western Himalaya have revealed winter and spring droughts in 1816 over large part of the western Himalaya (Yadav, 2013). Long-term tree-ring-based drought records from different parts of the Himalaya should help in understanding the impact of volcanic eruptions on climate over orography dominated mid-latitude regions. Our reconstruction further revealed droughts in successive years in 1921–1923 and 1966–1967 in Kumaun region. The SPI7-May was found to have remained above +1 from 1913 to 1916 and 1723–1724 indicating pluvial conditions. The dry and wet anomalies diagnosed from 3 and 5-year running mean of the reconstructed SPI series are indicated in Table 5. The SPI of 3-year mean indicated that the 1921–1923 were the driest and 1913–1915 the wettest in context of the past ~300 years. The 5-year mean SPI revealed droughts in 1920–1924, 1782–1786, 1812–1816, 1744–1748, 1964–1968 and pluvial in 1911–1915, 1723–1727, 1788–1792, 1758–1762 and 1733–1737 respectively.

To understand the regional signatures of climate in our SPI7-May reconstruction we performed field correlation analyses using CRU TS 3.22 gridded precipitation and temperature data (Harris et al., 2014) available through the KNMI Climate Explorer (http://climexp.knmi.nl; Oldenborgh and Burgers, 2005). The field correlations revealed spatial coherence in drought variability over Kumaun region with precipitation and temperature variations over the north-eastern region of India and Nepal (Fig. 8). A comparison

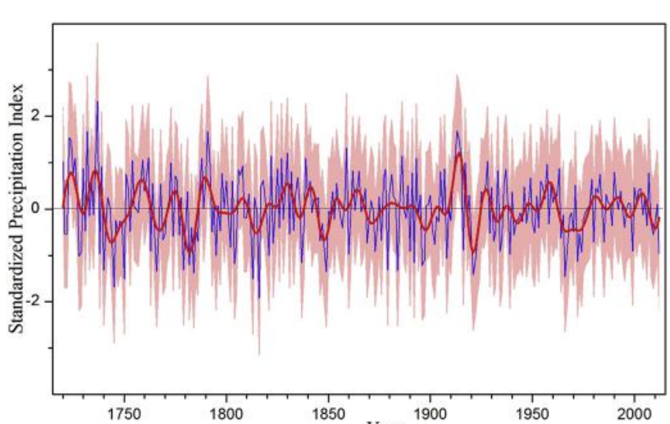

Fig. 7. SPI7-May reconstruction (1720–2012 CE) for Kumaun Himalaya overlaid with 10-year low pass filtered version (thick line). The pale red colour represents the 95% confidence interval of the tree-ring-based SPI estimates. (For interpretation of the references to colour in this figure legend, the reader is referred to the web version of this article.)

of drought records presented here with the boreal spring precipitation responsive ring-width chronology of birch (*Betula utilis*) from Central Nepal (Dawadi et al., 2013) revealed consistency in drought epochs in Kumaun and low growth indices of birch. Such a large-scale spatial coherence in tree-ring records from distant regions testifies the utility of our data in regional climatology. The droughts recorded during 1910s and 1960s in the Kumaun Himalaya are consistent with the tree-ring records from high elevation region of central Nepal Himalaya (Dawadi et al., 2013). The drought of 1999, which was widespread in the central Asia as a whole (Hoerling and Kumar, 2003) also occurred in the Kumaun and Nepal Himalaya as well (Sigdel and Ikeda, 2010). The droughts of 1974, 1985 recorded in our reconstruction were also widespread in Nepal largely due to winter precipitation failure (Sigdel and Ikeda, 2010). Though the Pacific and Indian Ocean temperature anomalies have been linked to the occurrence of such devastating droughts in the Himalayan region, the temporal instability in the relationship (Yadav, 2013) precludes reliable prediction of droughts in the region. As weather records from the orography dominated Himalayan region are very limited, high-resolution annually resolved proxies from a network of ecologically homogeneous sites should provide more robust and valuable data to understand drought variability in long-term perspective.

Weather records from different regions of westerly dominated western Himalaya show large spatial variability in winter and spring precipitation due to complex topography. The average precipitation in the westerly dominated region of the western Himalaya under the background influence of greenhouse warming is projected to show high spatial variability (IPCC, 2013). The Upper Indus basin under the dominant influence of westerly synoptic systems is projected to experience pluvial 21st century resulting in increased Indus flow (Ali et al., 2015). However, the projections for the western Nepal show increasing drought due to decreasing winter and spring season precipitation (Wang et al., 2013). Such a heterogeneous behaviour in winter/spring precipitation in the orography dominated western Himalayan region need to be investigated in long-term perspective and for this annually resolved large tree-ring data network from semi-arid to arid sites should provide valuable baseline data.

3.2. *Tree ring implications of drought records for Kumaun Himalaya*

Tree-ring chronologies from the western Himalayan region used to develop long-term drought records as a whole are very limited (Cook et al., 2010; Ram, 2012; Sano et al., 2012; Yadav, 2013). Using tree-ring chronology network from the monsoon Asia region including those from the western Himalaya, Cook et al. (2010) first developed June-July-August PDSI extending back to 1300 CE. The monsoon Asia drought atlas (MADA) developed by Cook et al. (2010) has revealed potential utility of data in understanding

Table 5
Individual years, 3-year and 5-year mean of SPI7-May as reconstructed from tree ring chronologies of Himalayan cedar from Kumaun Himalaya.

Individual years				3-year Mean				5-year Mean			
Dry		Wet		Dry		Wet		Dry		Wet	
Year	SPI	Year	SPI	Year	SPI	Year	SPI	Year	SPI	Year	SPI
1816	−1.92	1737	2.33	1921–1923	−1.08	1911–1913	1.14	1920–1924	−0.84	1911–1915	1.23
1745	−1.68	1913	1.69	1782–1784	−0.99	1735–1737	1.13	1782–1786	−0.82	1723–1727	1.03
1750	−1.50	1791	1.67	1972–1974	−0.86	1790–1792	1.12	1919–1923	−0.71	1788–1792	0.89
1813	−1.50	1732	1.67	1744–1746	−0.84	1724–1726	1.11	1812–1816	−0.71	1758–1762	0.77
1966	−1.45	1723	1.54	1966–1968	−0.84	1806–1808	0.83	1780–1784	−0.66	1733–1737	0.77

temporal and spatial variability in droughts and linkage with oceanic forcing. Later Ram (2012) using ring-width chronologies of *Abies pindrow* and *Picea smithiana* from Pahalgam, Jammu and Kashmir (34°02′N, 75°42′E, 2900 m asl) developed summer (April–September) PDSI extending back to 1820 CE. To understand relationship between ring-width chronologies of respective species with monthly PDSI variables Ram (2012) used PDSI data of one grid point (33°45′N, 73°45′E; 1229 m asl; Dai et al., 2004). The calibration model used to reconstruct mean summer (April–September) PDSI explained only 13% of the variance in observed PDSI data. Sano et al. (2012) further used δ^{18}O chronology of *Abies spectabilis* from Nepal to understand relationship with the mean PDSI series prepared using data available from single grid point close to tree-ring sites as well as three other grid points from distant locations in Indian plains (Sano et al., 2012). The δ^{18}O series on calibration with June-July-August-September (JJAS) mean PDSI data series explained 33.7% of the variance in observational PDSI data (1897–2000). More recently, Yadav (2013) developed October–May (OM) PDSI for a cold arid region of the western Himalaya by applying nested approach with network of ring-width chronologies of Himalayan cedar and neoza pine (*Pinus gerardiana*). In calibration model (1949–2005) individual nests explained ~35–38% of the variance in observed OM PDSI data (Yadav, 2013). In our opinion the weaker calibration statistics revealed thus far in PDSI reconstructions from the Himalayan region could be either due to the restricted availability of gridded PDSI data for the Himalayan region (Dai et al., 2004) and/or low spatial coverage of tree-ring data network (Ram, 2012; Sano et al., 2012; Yadav, 2013). However, in our present study the calibration statistics with SPI7-May was found to be much stronger even when only two site chronologies of Himalayan cedar from dry sites in the Kumaun Himalaya were used. In view of this, we strongly recommend that the SPI should be taken as an option to reconstruct droughts over different timescale in areas like the Himalaya where gridded PDSI data are spatially limited.

3.3. SPI and wheat-barley productivity in the Kumaun Himalaya

Wheat and barley are the major cereal crops in hill regions of the Kumaun Himalaya where prevalence of cool climate and long growing season is very conducive for cultivation of these crops. However, the productivity of these crops is highly vulnerable to fluctuations in precipitation as major part of the cropping area, usually on terraced farms, are rainfed due to non-availability of water and terrain constrains. As a whole, ~89% of the agriculture in the Kumaun region is rainfed and the remaining fraction of irrigated area restricted to valleys (Anonymous, 2012). The rainfed nature of agricultural practices in hilly terrains makes it vulnerable to soil moisture fluctuations, which are a function of precipitation over a period of several months. To understand if SPI, a metric of drought, could be used to quantify drought impact on rabi crop production we correlated different months SPI with wheat and barley productivity data for Almora in the Kumaun Himalaya. The crop productivity data available with us for Almora ranged from 1974 to 2010 with stray records of 1960s. We found that the SPI7-May showed significant correlation with wheat and barley production ($r = 0.60$, 1974–2010, two-tailed $p = 0.0001$) (Fig. 9). However, we noted that the SPI7-April showed somewhat stronger correlation with wheat and barley production ($r = 0.69$, 1974–2010, two-tailed $p = 0.0001$). The reconstructed SPI7-May indicated still weaker correlation with wheat and barley production ($r = 0.44$, 1974–2010, two-tailed $p = 0.0082$), which could be possibly improved further with the development of more robust reconstructions by using larger tree-ring data network in the calibration model. The decreased correlation between SPI7-May and wheat-barley productivity compared to SPI7-April could be

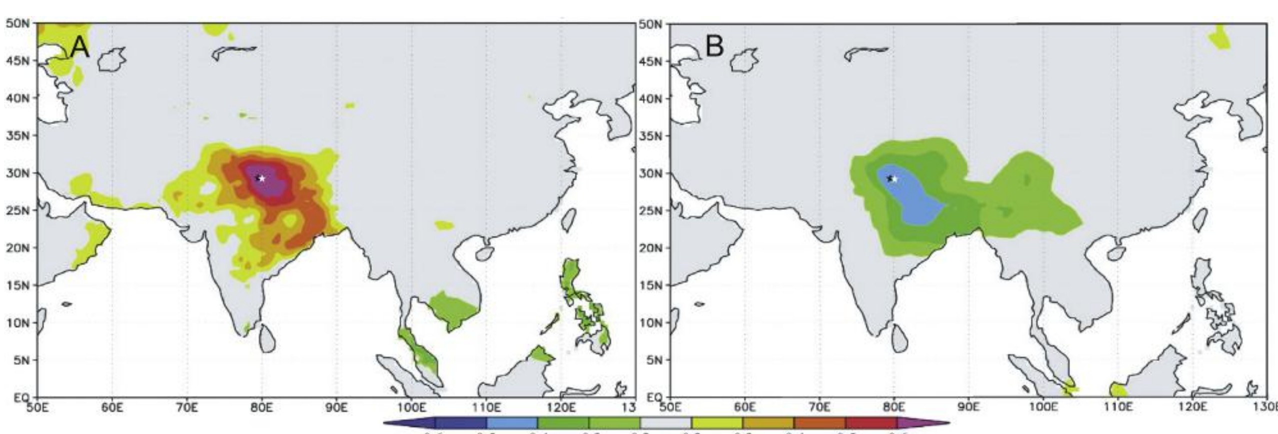

Fig. 8. Spatial correlation between reconstructed SPI7-May and CRU TS 3.22 for 1902–2012; A. with precipitation, and B. with temperature (http://climexp.knmi.nl, Oldenborgh and Burgers, 2005). Dark filled and white stars represent Jageshwar and Gangolihat tree-ring collection sites in Kumaun Himalaya.

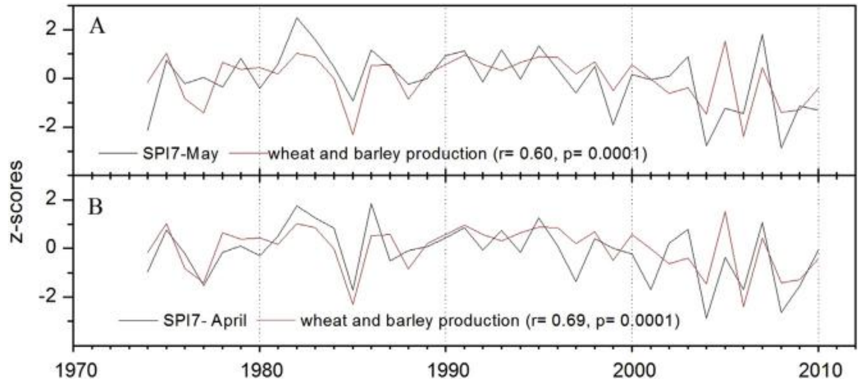

Fig. 9. Wheat-barley productivity and SPI data (1974–2010) plotted together. The data were normalized with respect to 1974–2010 mean and standard deviation (wheat mean productivity 961.8 kg/ha and standard deviation 175.2 kg/ha; barley mean productivity 948.9 kg/ha and standard deviation 197.4 kg/ha); A. SPI7-May and wheat-barley productivity, B. SPI7-April and wheat-barley productivity.

largely for the reason that these crops mature and get usually harvested in May, except in case of high elevation regions where ripening of crops could be as late as in June.

We compared drought records developed from tree-ring chronologies with the periods of food shortages reported in the Kumaun region and observed that many of the drought indices were associated with rabi crop failures. Interestingly we noted that the low SPI indices (<1) indicating droughts recorded in 1890, 1892, 1896, 1897 were associated with rabi crop failures in Kumaun (Anonymous, 1898). The rabi crop failure in 1908 in Kumaun and Garhwal (Walton, 1910) was also consistent with negative SPI7-May values in observational as well as tree-ring-based reconstruction. The negative SPI7-May values during 1920–1924 revealed persistent droughts in the Kumaun region, which could have caused failure of rabi crop production. Interestingly, unprofitable farming of local farming community during this multiyear drought period is found to be consistent with the reduction in cultivation area of wheat and barley in the Kumaun region (Mittal, 1986) and rise in food grain prices (Anonymous, 1981). The food scarcity in the Kumaun region also occurred in drought year of 1939 due to rabi crop failure (Das, 1999). The SPI values indicating droughts in the Kumaun during 1963–1974 were also associated with the severe reduction in rabi crop production. In such a protracted drought period the wheat-barley production was the lowest especially in 1966 (Anonymous, 1971). The cultivation of wheat and barley was not preferred by the farming community during such an extended drought period of 1960s and even the utilization of improved quality seeds of these crops dropped in Almora District during this period (Anonymous, 1971). The winter droughts of 2008–09 in Kumaun were also found to be consistent with droughts in western Nepal when wheat and barley production dropped by 50% in comparison to the previous year (Wang et al., 2013). The winter–spring precipitation has shown downward trend since 1995 in western Nepal which had serious agro-economic implications (Wang et al., 2013). Viewing on such a tight linkage between SPI records and production of wheat and barley in hill regions, it is hoped that larger tree-ring data network from moisture stressed sites in the Kumaun Himalaya should provide valuable data base to understand temporal variability in rabi crop productivity associated with droughts in long-term perspective.

4. Conclusions

We developed SPI7-May reconstruction (1720–2012 CE) using tree-ring width chronologies of Himalayan cedar developed from two ecologically homogeneous moisture stressed sites in the Kumaun Himalaya, India. The SPI7-May reconstruction developed for the Kumaun Himalaya, which captured 60% of the variance in observational SPI data in calibration model (1902–1967), is the strongest thus far from the Indian region. On the basis of such a strong calibration statistics we recommend that the tree-ring records from moisture stressed sites in the Kumaun Himalaya should be used to develop long-term SPI records to understand temporal and spatial variability in droughts.

The reconstructed SPI7-May data revealed high year-to-year variability. The most revealing multi-year droughts occurred in 1920–1924, 1782–1786, 1812–1816, 1744–1748, 1964–1968 and pluvial in 1911–1915, 1723–1727, 1788–1792, 1758–1762 and 1733–1737 respectively. The SPI7-May records developed for the Kumaun region further revealed significant relationship with the productivity of wheat and barley crops in Almora, close to our tree-ring study sites. The rabi crop failures and food scarcity in the Kumaun region were found to be linked with the drought years recorded in observational and reconstructed SPI7-May series. Such a relationship between drought indices and wheat-barley productivity revealed the potential utility of tree-ring data in understanding the variability in food-grain production in rainfed regions of the Kumaun Himalaya in long-term perspective.

Acknowledgements

The research work was partly supported by financial grants from ISRO-GBP to RRY and BSK. The Department of Agriculture, Government of Uttar Pradesh, Lucknow and Uttarakhand very kindly provided the crop productivity data. Authors express their sincere thanks to two anonymous reviewers for their critical suggestions, which improved the earlier version of the text to a great extent.

References

Aggarwal, R.K., 2013. Effect of rainfall on cropping pattern in mid Himalayan region. Afr. J. Environ. Sci. Technol. 7, 634–640.

Ali, S., Li, D., Congbin, F., Khan, F., 2015. Twenty first century climatic and hydrological changes over Upper Indus Basin of Himalayan region of Pakistan. Environ. Res. Lett. 10 http://dx.doi.org/10.1088/1748-9326/10/1/014007.

Anonymous, 1898. Report of the Indian Famine Commission 1898. Printed at the Govt. Central Printing Office, Shimla.

Anonymous, 1971. Season and Crop Report of Uttar Pradesh, 1965–66. Published by the board of revenue (Land reforms), Uttar Pradesh Lucknow. Superintendent Printing and Stationery, Allahabad, Uttar Pradesh, India.

Anonymous, 1981. Uttar Pradesh District Gazetteers: Almora. Government Press, Lucknow.

Anonymous, 2009. Agricultural Statistics at a Glance. Ministry of Agriculture, New Delhi.

Anonymous, 2012. Uttarakhand State Action Plan for Climate Change. Government of Uttarakhand.

Biondi, F., Waikul, K., 2004. DENDROCLIM2002: a C++ program for statistical calibration of climate signals in tree-ring chronologies. Comput. Geosci. 30, 303–311.

Black, B.A., Sydeman, W.J., Frank, D.C., Griffin, D., Stahle, D.W., García-Reyes, M., Rykaczewski, R.R., Bograd, S.J., Peterson, W.T., 2014. Six centuries of variability and extremes in a coupled marine-terrestrial ecosystem. Science 345, 1498–1502.

Burnette, D.J., Stahle, D.W., 2013. Historical perspective on the dust bowl drought in the central United States. Clim. Change 116, 479–494.

Cook, E.R., 1985. A Time Series Approach to Tree-ring Standardization. Ph.D. thesis. University of Arizona, Tucson, Arizona, USA.

Cook, E.R., Peters, K., 1981. The smoothing spline: a new approach to standardizing forest interior tree-ring series for dendroclimatic studies. Tree-Ring Bull. 41, 45–53.

Cook, E.R., Kairiukstis, L.A. (Eds.), 1990. Methods of Dendrochronology: Applications in the Environmental Sciences. Kluwer Academic Publishers, Netherlands.

Cook, E.R., Peters, K., 1997. Calculating unbiased tree-ring indices for the study of climatic and environmental change. Holocene 7, 361–370. http://dx.doi.org/10.1177/095968369700700314.

Cook, E.R., Krusic, P.J., Jones, P.D., 2003. Dendroclimatic signals in long tree-ring chronologies from the Himalayas of Nepal. Int. J. Climatol. 23, 707–732.

Cook, E.R., Woodhouse, C.A., Eakin, C.M., Meko, D.M., Stahle, D.W., 2004. Long-term aridity changes in the western United States. Science 306, 1015–1018.

Cook, E.R., Seager, R., Cane, M.A., Stahle, D.W., 2007. North American drought: reconstructions, causes, and consequences. Earth Sci. Rev. 81, 93–134.

Cook, E.R., Anchukaitis, K.J., Buckley, B.M., D'Arrigo, R.D., Jacoby, G.C., Wright, W.E., 2010. Asian monsoon failure and megadrought during the last millennium. Science 328, 486–489.

Dai, A., Trenberth, K.E., Qian, T., 2004. A global dataset of Palmer drought severity index for 1870-2002: relationship with soil moisture and effects of surface warming. J. Hydrometeorol. 5, 1117–1130.

Das, B., 1999. Uttar Pradesh District Gazetteers, Nainital. Published by the Government of Uttar Pradesh, Printed at the government press, Allahabad.

Davi, N.K., Jacoby, G.C., Curtis, A.E., Baatarbileg, N., 2006. Extension of drought records for Central Asia using tree rings: West-Central Mongolia. J. Clim. 19, 288–299.

Dawadi, B., Liang, E., Tian, L., Devkota, L.P., Yao, T., 2013. Pre-monsoon precipitation signal in tree-rings of timberline *Betula utilis* in the central Himalayas. Quat. Int. 283, 72–77.

Edwards, D.C., McKee, T.B., 1997. Characteristics of 20th Century Drought in the United States at Multiple Time Scales. Climatology Report 97–2. Department of Atmospheric Science, Colorado State University, Fort Collins, Colorado.

Esper, J., 2000. Long-term tree-ring variations in Juniperus at the upper timber-line in the Karakorum (Pakistan). Holocene 10, 253–260.

Esper, J., Frank, D., Buntgen, U., Verstege, A., Luterbacher, J., Xoplaki, E., 2007. Long-term drought severity variations in Morocco. Geophys. Res. Lett. 34, L17702. http://dx.doi.org/10.1029/2007GL030844.

Fritts, H.C., 1976. Tree-rings and Climate. Academic Press, London.

Gadgil, S., Kumar, K.R., 2006. The Asian monsoon- agriculture and economy. In: Wang, B. (Ed.), The Asian Monsoon. Springer, Berlin Heidelberg, pp. 651–683.

GOI, 1976. Report of the National Commission on Agriculture. Ministry of Agriculture and Irrigation, New Delhi.

Griffin, D., Anchukaitis, K.J., 2014. How unusual is the 2012–2014 California drought? Geophys. Res. Lett. 41 http://dx.doi.org/10.1002/2014GL062433.

Gupta, A.K., Tyagi, P., Sehgal, V.K., 2011. Drought disaster challenges and mitigation in India: strategic appraisal. Curr. Sci. 100, 1795–1806.

Harris, I., Jones, P.D., Osborn, T.J., Lister, D.H., 2014. Updated high-resolution grids of monthly climatic observations-the CRU TS3.10 dataset. Int. J. Climatol. 34, 623–642.

Hoerling, M., Kumar, A., 2003. Perfect Ocean for drought. Science 299, 691–694.

IPCC, 2013. In: Stocker, T.F., Qin, D., Plattner, G.-K., Tignor, M., Allen, S.K., Boschung, J., Nauels, A., Xia, Y., Bex, V., Midgley, P.M. (Eds.), Climate Change 2013: the Physical Science Basis. Contribution of Working Group I to the Fifth Assessment Report of the Intergovernmental Panel on Climate Change. Cambridge University Press, Cambridge and New York.

Jameson, J., 1820. Report on the Epidemik Cholera Morbus, as it Visited the Territories Subject to the Presidency of Bengal in the Years 1817, 1818 and 1819. Government Gazette Press, Calcutta, p. 325.

Joseph, R., Zeng, N., 2009. Seasonally modulated tropical drought induced by volcanic aerosol. J. Clim. 24, 2045–2060.

Keyantash, J., Dracup, J.A., 2002. The quantification of drought: an evaluation of drought indices. Bull. Am. Meteor. Soc. 83, 1167–1180.

Li, J., Gou, X., Cook, E.R., Chen, F., 2006. Tree-ring based drought reconstruction for the central Tien Shan area in northwest China. Geophys. Res. Lett. 33, L07715. http://dx.doi.org/10.1029/2006GL025803.

Li, J., Chen, F., Cook, E.R., Goua, X., Zhang, Y., 2007. Drought reconstruction for north central China from tree rings: the value of the Palmer drought severity index. Int. J. Climatol. 27, 903–909.

Liang, E., Liu, X., Yuan, Y., Qin, N., Fang, X., Huang, L., Zhu, H., Wang, L., Shao, X., 2006. The 1920s drought recorded by tree rings and historical documents in the semi-arid and arid areas of northern China. Clim. Change 79, 403–432.

Lloyd-Hughes, B., Saunders, M.A., 2002. A drought climatology for Europe. Int. J. Climatol. 22, 1571–1592.

McKee, T.B., Doesken, N.J., Kleist, J., 1993. The relationship of drought frequency and duration to time scales. In: Proceeding of the 8th Conference on Applied Climatology. American Meteorological Society, Boston, pp. 179–184.

Meko, D.M., Stahle, D.W., Griffin, D., Knight, T.A., 2011. Inferring precipitation-anomaly gradients from tree rings. Quat. Int. 235, 89–100.

Mishra, A.K., Singh, V.P., 2010. A review of drought concepts. J. Hydrol. 391, 202–216.

Mittal, A.K., 1986. British Administration in Kumaun Himalayas: a Historical Study. Mittal Publications, Delhi.

Nagarajan, S., 2005. Can India produce enough wheat even by 2020? Curr. Sci. 89, 1467–1471.

Oldenborgh, G.J., Burgers, G., 2005. Searching for decadal variations in ENSO precipitation teleconnections. Geophys. Res. Lett. 32, L15701,. http://dx.doi.org/10.1029/2005GL023110.

Palmer, W.C., 1965. Meteorological Drought. Res. Paper No.45. Dept. of Commerce, Washington, D.C, p. 58.

Písek, J., Brázdil, R., 2006. Responses of large volcanic eruptions in the instrumental and documentary climatic data over Central Europe. Int. J. Climatol. 26, 4439–4459.

Ram, S., 2012. Tree growth–climate relationships of conifer trees and reconstruction of summer Palmer Drought Severity Index at Pahalgam in Srinagar, India. Quat. Int. 254, 152–158.

Rinn, F., 1996. TSAP-win Time Series Analysis and Presentation for Dendrochronology and Related Applications, Version 0.53 for Microsoft Windows. Rinn Tech, Heidelberg, Germany, p. 110.

Robock, A., 2000. Volcanic eruptions and climate. Rev. Geophys. 38, 191–219.

Sano, M., Ramesh, R., Sheshshayee, M.S., Sukumar, R., 2012. Increasing aridity over the past 223 years in the Nepal Himalaya inferred from a tree-ring $\delta^{18}O$ chronology. Holocene 22, 809–817.

Self, S., Gertisser, R., Thordarson, T., Rampino, M.R., Wolff, J.A., 2004. Magma volume, volatile emissions, and stratospheric aerosols from the 1815 eruption of Tambora. Geophys. Res. Lett. 31, L20608 doi:1029/2004GL020925.

Shao, X.M., Xu, Y., Yin, Z.-Y., Liang, E., Zhu, H., Wang, S., 2010. Climatic implications of a 3585-year tree-ring width chronology from the northeastern Qinghai-Tibetan Plateau. Quat. Sci. Rev. 29, 2111–2122.

Sheppard, P.R., Tarasov, P.E., Graumlich, L.J., Heussner, K.-U., Wagner, M., Sterle, H.O., Thompson, L.G., 2004. Annual precipitation since 515 BC reconstructed from living and fossil juniper growth of northeastern Qinghai Province, China. Clim. Dyn. 23, 869–881.

Sigdel, M., Ikeda, M., 2010. Spatial and temporal analysis of drought in Nepal using standardized precipitation index and its relationship with climate indices. J. Hydrol. Meteorol. 7, 59–74.

Singh, J., Yadav, R.R., 2007. Dendroclimatic potential of millennium-long ring-width chronology of *Pinus gerardiana* from Himachal Pradesh, India. Curr. Sci. 93, 833–836.

Singh, J., Yadav, R.R., Dubey, B., Chaturvedi, R., 2004. Millennium-long ring-width chronology of Himalayan cedar from Garhwal Himalaya and its potential in climate change studies. Curr. Sci. 86, 590–593.

Stahle, D.W., Fye, F.K., Cook, E.R., Griffin, R., 2007. Tree-ring reconstructed megadroughts over North America since A. D. 1300. Clim. Change 83, 133–149.

Stahle, D.W., Griffin, R.D., Meko, D.M., Therrell, M.D., Edmondson, J.R., Cleaveland, M.K., Stahke, L.N., Burnette, D.J., Abatzoglou, J.T., Redmond, K.T., Dettinger, M.D., Cayan, D.R., 2013. The ancient blue oak woodlands of California: longevity and hydroclimatic history. Earth Interact. 17, 1–23.

Sun, J., Liu, Y., 2013. Drought variations in the middle Qilian Mountains, northeast Tibetan Plateau over the last 450 years as reconstructed from tree rings. Dendrochronologia 31, 279–285.

Touchan, R., Gary, F., Hughes, M.K., Erkan, N., 2005. Standardized precipitation index reconstructed from Turkish tree-ring widths. Clim. Change 72, 339–353.

Touchan, R., Anchukaitis, K.J., Meko, D.M., Attalah, S., Baisan, C., Aloui, A., 2008. Long term context for recent drought in northwestern Africa. Geophys. Res. Lett. 35, L13705,. http://dx.doi.org/10.1029/2008GL034264.

Touchan, R., Anchukaitis, K.J., Meko, D.M., Sabir, M., Attalah, S., Aloui, A., 2011. Spatiotemporal drought variability in northwestern Africa over the last nine centuries. Clim. Dyn. 37, 237–252.

Treydte, K.S., Schleser, G.H., Helle, G., Frank, D.C., Winiger, M., Haug, G.H., Esper, J., 2006. The twentieth century was the wettest period in northern Pakistan over the past millennium. Nature 440, 1179–1182.

Vicente-Serrano, S.M., Begueria, S., Lopez-Moreno, J.I., Angulo, M., Kenawy, A.El, 2010. A new global 0.5° gridded dataset (1901–2006) of a multiscalar drought index: comparison with current drought index datasets based on the Palmer Drought Severity Index. J. Hydrometeorol. 11, 1033–1043.

Walton, H.G., 1910. A Gazetteer of Garhwal Himalaya. Natraj Publishers, Dehradun.

Wang, S.-Y., Yoon, J.-H., Gillies, R.R., Cho, C., 2013. What caused the winter drought in Western Nepal during recent years? J. Clim. 26, 8241–8256.

Wigley, T.M.L., Briffa, K.R., Jones, P.D., 1984. On the average value of correlated time series with applications in dendroclimatology and hydrometeorology. Int. J. Climatol. 8, 33–54.

Wilhite, D.A., 2000. Drought as a natural hazard: concepts and definitions (Chapter 1). In: Wilhite, D.A. (Ed.), Drought: a Global Assessment. Hazards and Disasters: a Series of Definitive Major Works, Edited by A.Z. Keller. Routledge Publishers, London, UK.

WMO, 2012. Standardized Precipitation Index User Guide. WMO No. 1090, Geneva.

Woodhouse, C., Overpeck, J., 1998. 2000 years of drought variability in the central United States. Bull. Am. Meteor. Soc. 79, 2693–2714.

Woodhouse, C.A., Meko, D.M., MacDonald, G.M., Stahle, D.W., Cook, E.R., 2010. A 1200-year perspective of 21st century drought in southwestern North America. Proc. Natl. Acad. Sci. 107, 21283–21288.

Yadav, R.R., 2011a. Tree-ring evidence of 20th century precipitation surge in monsoon shadow zone of western Himalaya, India. J. Geophys. Res. Atmos. 116 http://dx.doi.org/10.1029/2010JD014647.
Yadav, R.R., 2011b. Long-term hydroclimatic variability in monsoon shadow zone of western Himalaya, India. Clim. Dyn. 36, 1453–1462.
Yadav, R.R., 2012. Over two millennia long ring-width chronology of Himalayan pencil cedar from Western Himalaya, India. Curr. Sci. 103, 1279–1280.
Yadav, R.R., 2013. Tree ring-based seven-century drought records for the western Himalaya, India. J. Geophys. Res. Atmos. 118, 4318–4325.
Yadav, R.R., Park, W.-K., Bhattacharyya, A., 1999. Spring temperature variations in western Himalaya, India, as reconstructed from tree-rings: A.D. 1390e1987. Holocene 9, 85–90.
Yadav, R.R., Singh, J., 2002. Tree-ring-based spring temperature patterns over the past four centuries in western Himalaya. Quat. Res. 57, 299–305.
Yadav, R.R., Park, W.-K., Singh, J., Dubey, B., 2004. Do the western Himalayas defy global warming? Geophys. Res. Lett. 31, L17201,. http://dx.doi.org/10.1029/2004GL020201.
Yadav, R.R., Singh, J., Dubey, B., Mishra, K.G., 2006. A 1584-year ring width chronology of juniper from Lahul, Himachal Pradesh: prospects of developing millennia long climate records. Curr. Sci. 90, 1122–1126.
Yadav, R.R., Braeuning, A., Singh, J., 2011. Tree ring inferred summer temperature variations over the last millennium in western Himalaya, India. Clim. Dyn. 36, 1545–1554.
Yadav, R.R., Misra, K.G., Kotlia, B.S., Upreti, N., 2014a. Age of Himalayan cedar outside its natural home in the Himalayas. Curr. Sci. 106, 932–935.
Yadav, R.R., Misra, K.G., Kotlia, B.S., Upreti, N., 2014b. Premonsoon precipitation variability in Kumaun Himalaya, India over a perspective of ~300 years. Quat. Int. 325, 213–219.
Yang, B., Qin, C., Shi, F., Sonechkin, M., 2012. Tree ring-based annual streamflow reconstruction for the Heihe River in arid northwestern China from AD 575 and its implications for water resource management. Holocene 22, 773–784.
Yang, B., Kang, S., Ljungqvist, F.C., He, M., Zhao, Y., Qin, C., 2014a. Drought variability at the northern fringe of the Asian summer monsoon region over the past millennia. Clim. Dyn. 43, 845–859.
Yang, B., Qin, C., Wang, J., He, M., Melvin, T.M., Osborn, T.J., Briffa, K.R., 2014b. A 3,500-year tree-ring record of annual precipitation on the northeastern Tibetan Plateau. Proc. Natl. Acad. Sci. http://dx.doi.org/10.1073/pnas.1319238111.
Yin, Z.-Y., Shao, X., Qin, N., Liang, E., 2008. Reconstruction of a 1436-year soil moisture and vegetation water use history based on tree-ring widths from Qilian junipers in northeastern Qaidam Basin, northwestern China. Int. J. Climatol. 28, 37–53.
Zhang, Y., Tian, Q., Gou, X., Chen, F., Leavitt, S.W., Wang, Y., 2011. Annual precipitation reconstruction since AD 775 based on tree rings from the Qilian Mountains, northwestern China. Int. J. Climatol. 31, 371–381.